OPEN

PRS GLOBAL OPEN

IDEAS AND INNOVATIONS

Reconstructive

High-end versus Low-end Thermal Imaging for Detection of Arterial Perforators

Magnús Pétur Bjarnason Obinah, MD*
Monica Nielsen, DVM†
Lisbet Rosenkrantz Hölmich, DMSc, MD*‡

Background: Thermal imaging was first reported as a method for detection of arterial perforators in 1968 and has since been shown to be an extremely accurate way to assess perforators with an audible Doppler signal, using high-end professional thermal cameras. This technology has recently become easily accessible with the advent of smartphone-compatible, low-end thermal cameras. Several groups have reported on the use of these devices in the pre-, intra-, and postoperative phase, yet there have been few attempts to validate them against existing methods or compare them with high-end thermal cameras.

Methods: The aim of this study was to compare a low-end smartphone-compatible thermal camera, the FLIR ONE Pro (ONEPro), priced US $400, with a high-end thermal camera the FLIR A35sc (A35sc), priced US $5000, for the detection of arterial perforators on the anterolateral thigh, using a handheld Doppler and Color Doppler Ultrasound to verify the results.

Results: We examined 23 thighs in 13 healthy volunteers and identified a total of 779 hotspots using both cameras. The A35sc identified on average 33.5 hotspots per thigh. The ONEPro identified on average 31.5 hotspots per thigh. Using a handheld Doppler, we confirmed 95.9% of hotspots identified with the ONEPro and 95.8% of hotspots identified with the A35sc. Using Color Doppler Ultrasound, we confirmed 95% of hotspots identified using the ONEPro and 94.9% of hotspots identified with the A35sc.

Conclusion: While the high-end camera identified slightly more hotspots, verification data were very similar for the 2 cameras, and for clinical purposes these differences are negligible. *(Plast Reconstr Surg Glob Open 2020;8:e3175; doi: 10.1097/GOX.0000000000003175; Published online 4 November 2020.)*

INTRODUCTION

Localization of arterial perforators[1] has been described using various modalities, including handheld Doppler (HHD), Color Doppler Ultrasound (CDU), computed tomography angiography (CTA), and magnetic resonance angiography.[2]

HHD is an inexpensive and transportable, but time-consuming, poorly validated,[3] and prone to false-negative and false-positive results, especially in thin or obese individuals.[4,5] CDU provides information on localization, diameter, and flow, but is time-consuming and operator-dependent, requiring a radiologist or a trained specialist,[6] making it expensive and less accessible.[2] CTA, the current gold standard, and magnetic resonance angiography are expensive, time-consuming, and not suitable for intraoperative use, both expose patients to the risk of intravenous contrast fluids and CTA to ionizing radiation as well.[2,7,8] Indocyanine green, a reliable and easy method for perforator identification and selection,[9,10] allows only short recordings, is invasive, and carries a slight risk of adverse reaction.[11]

Infrared thermography is the detection of infrared radiation and production of a thermogram for

*From the *Department of Plastic Surgery, Herlev and Gentofte University Hospital, Copenhagen, Denmark; †Faculty of Health and Medical Science, University of Copenhagen, Copenhagen, Denmark; and ‡Department of Clinical Medicine, University of Copenhagen, Copenhagen, Denmark.*

Received for publication February 20, 2020; accepted August 14, 2020.

DOI: 10.1097/GOX.0000000000003175

Disclosure: *The authors have no financial interest to declare in relation to the content of this article. The FLIR A35sc camera was lent to the investigators free of charge by a local retailer (Altoo Measurement Science ApS, Hørsholm, Denmark) for the purpose of this study.*

Related Digital Media are available in the full-text version of the article on www.PRSGlobalOpen.com.

visualizing variations in temperature, typically using a gradient of colors (**see figure 1, Supplemental Digital Content 1**, which shows a thermogram using 3 different color palettes, **http://links.lww.com/PRSGO/B489**). Thermography was first reported as a diagnostic aid in 1956, when Lawson noticed a higher skin temperature over a tumor in a patient's breast.[12] In 1968, Arai and Fukuda[13] visualized higher skin temperatures, referred to as "hotspots," corresponding to the locations of arterial perforators.

In 2013, Sheena et al[14] reported using a high-end thermal camera for localizing arterial perforators and confirmed 97% of 757 hotspots using HHD, and an animal study, by combining high-end thermography with CDU for perforator mapping, reported a good correlation with intraoperative findings.[15] In 2016, Hardwicke et al[16] described using a low-end, smartphone-compatible thermal camera, the FLIR ONE for pre-, intra-, and postoperative use, concluding that it provided a low-cost alternative that could identify hotspots for confirmation using HHD. Other authors have reported positive results with low-end thermal cameras,[17–21] and a study comparing the FLIR ONE with CTA for identification of arterial perforators reported high concordance between the methods.[22]

Despite increasing use of low-end thermography, there is a lack of validation data.[23,24] The purpose of this study was to compare a low-end and a high-end thermal camera for detection of arterial perforators, using HHD and CDU to validate the results.

PATIENTS AND METHODS

A study of healthy, consenting volunteers was carried out at Herlev Gentofte Hospital, Denmark. This study was submitted to the board of medical ethics (no. 61779).

We compared the FLIR ONE Pro (Flir-Systems, Wilsonville, Ore.) (ONEPro) with the FLIR A35sc (Flir-Systems) (A35sc). The ONEPro is a low-end that requires connection to a smartphone running a FLIR application, with a 160 × 120 thermal resolution, a thermal sensitivity/noise-equivalent temperature difference (NETD) of 0.07°C/70 mK, priced $400. The ONEPro has a multispectral dynamic imaging (MSX), where 2 images are taken simultaneously, 1 with a built-in digital camera and 1 with the thermal camera, and visible light details extracted from the digital image are embossed over the thermal images in real time. The A35sc is a scientific thermal camera, which requires connection via Gigabit Ethernet to a computer running FLIR analysis software, with a 320 × 256 thermal resolution and a thermal sensitivity/NETD of <0.05°C/50 mK, priced $5000.

The room was kept at 23°C. Volunteers were placed in a supine position and thigh areas exposed for 5 minutes before imaging. A fixed section of the anterolateral thigh was marked, and imaging was performed within this border, first using the ONEPro, then the A35sc, both held at 70 cm distance to the skin (Fig. 1). Hotspots, defined as localized thermal signatures with temperatures ≈1–2°C higher than the surrounding skin, were marked corresponding to the identifying cameras, and digital photography of the entire area was performed.

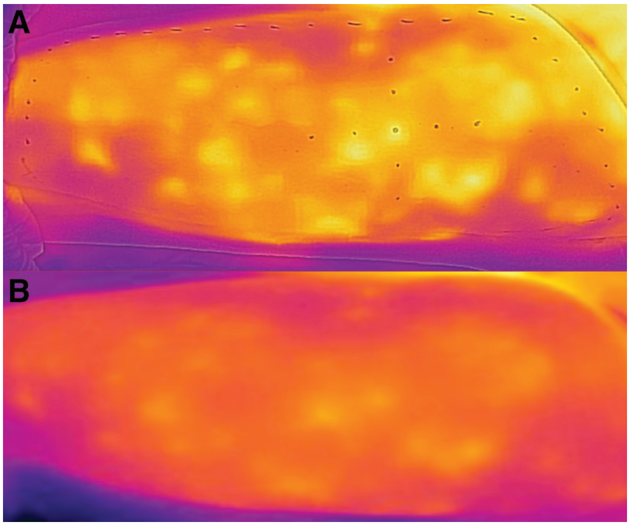

Fig. 1. Thermogram of a marked left thigh area, with matching temperature range (TR) settings. A, FLIR ONE Pro with MSX. B, FLIR AS35sc.

HHD was performed using a Huntleigh D900 (Huntleigh, Cardiff, UK). A positive result was defined as an audible pulsation corresponding to a marking. CDU was performed using a BK Flex Focus 500 (BK Ultrasound, Richmond, Canada). A positive result was defined as visible pulsatile arterial flow corresponding to markings, traceable to the underlying fascia (**see figure 2, Supplemental Digital Content 2**, which shows a CDU image of a perforator traveling from the muscle fascia to the skin, **http://links.lww.com/PRSGO/B490**) (**see Video 1 [online]**, which demonstrates the CDU scanning process).

RESULTS

We examined 23 thighs in 13 healthy volunteers, 8 men and 5 women, with a mean age of 39.9 years (26–60) and mean body mass index (BMI) of 25.2 kg/m^2 (16.70–32.00). Verification results are summarized in Table 1. We found a significant association between low BMI and the number of CDU negative hotspots, which constituted 29 of 404 (7.2%) hotspots identified in thighs where BMI < 25, and 12 of 375 (3.2%) hotspots in thighs where BMI ≥ 25, χ^2 (1, N = 779) = 6.1729, $P = 0.013$.

DISCUSSION

The A35sc identified 6.3% additional hotspots, possibly due to higher thermal sensitivity allowing detection of smaller vessels. High-end thermal cameras are expensive, nonmobile, and require specialized software, whereas low-end smartphone-compatible cameras are cheap, small, and easy to use. These devices were not designed for clinical use,[25] and certain settings should be understood before use. Hotspots represent small variations in temperature, which may be obscured if the camera automatically adjusts the temperature range based on the lowest and highest temperatures within its field of view. We therefore recommend locking temperature range to a region of interest (Fig. 2). When using MSX mode, parallax may cause a difference in the apparent position of visible-light objects

Table 1. Confirmation Data for Hotspots Identified with Each Camera Separately and for Hotspots Identified with Both Cameras

Thermal Camera	Identified	Mean per Thigh	Doppler Confirmed	CDU Confirmed	Doppler and CDU Confirmed
FLIR ONE Pro	724 (92.9%)	31.5 (15–47)	694 (95.9%)	688 (95.0%)	661 (91.3%)
FLIR AS35sc	770 (98.8%)	33.5 (12–51)	738 (95.8%)	731 (94.9%)	701 (91.0%)
ONE Pro and AS35sc	715 (91.8%)	31.1 (12–47)	686 (95.9%)	681 (95.2%)	654 (91.5%)
Total	779 (100%)				

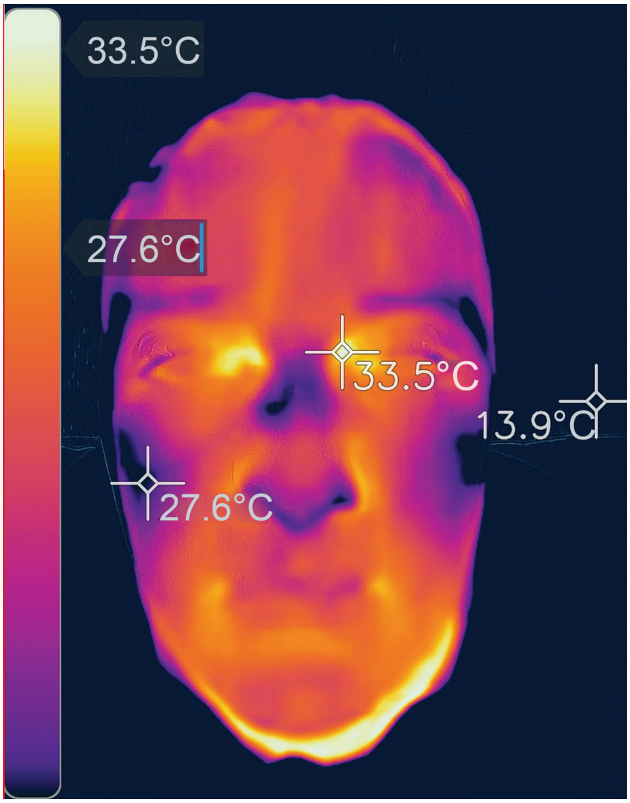

Fig. 2. Thermogram of the face using the iron palette, where temperature range (TR) is set from 27.6°C to 33.5°C corresponding to the coldest and warmest points found within the region of interest (ROI).

relative to the thermographic image. The Distance Slider should be adjusted according to the distance between the camera and the skin surface (**see Video 2 [online]**, which demonstrates the imaging process using the ONEPro). Hotspots should be examined with CDU to determine the size and path of the underlying vessel.

Of note, some authors recommend using dynamic infrared thermography, where skin is cooled before thermal imaging, for identification of cutaneous perforators with high reperfusion rates, which may indicate increased vessel flow and diameter.[26–35]

CONCLUSIONS

Verification data were very similar for both cameras. Low BMI was associated with more false-positive hotspots. Further validation against CTA or operative exploration should be performed.

Magnús Pétur Bjarnason Obinah, MD
Department of Plastic Surgery
Herlev Ringvej 75
2730 Herlev, Denmark
E-mail: mpb@obinah.com

REFERENCES

1. Taylor GI, Palmer JH. The vascular territories (angiosomes) of the body: experimental study and clinical applications. *Br J Plast Surg*. 1987;40:113–141.
2. Mathes DW, Neligan PC. Preoperative imaging techniques for perforator selection in abdomen-based microsurgical breast reconstruction. *Clin Plast Surg*. 2010;37:581,ix–591, xi.
3. Stekelenburg CM, Sonneveld PM, Bouman MB, et al. The hand held Doppler device for the detection of perforators in reconstructive surgery: what you hear is not always what you get. *Burns*. 2014;40:1702–1706.
4. Shaw RJ, Batstone MD, Blackburn TK, et al. The anterolateral thigh flap in head and neck reconstruction: “pearls and pitfalls”. *Br J Oral Maxillofac Surg*. 2010;48:5–10.
5. Yu P, Youssef A. Efficacy of the handheld Doppler in preoperative identification of the cutaneous perforators in the anterolateral thigh flap. *Plast Reconstr Surg*. 2006;118:928–933; discussion 934.
6. Taylor GI, Doyle M, McCarten G. The Doppler probe for planning flaps: anatomical study and clinical applications. *Br J Plast Surg*. 1990;43:1–16.
7. Rozen WM, Stella DL, Bowden J, et al. Advances in the pre-operative planning of deep inferior epigastric artery perforator flaps: magnetic resonance angiography. *Microsurgery*. 2009;29:119–123.
8. Rozen WM, Ribuffo D, Atzeni M, et al. Current state of the art in perforator flap imaging with computed tomographic angiography. *Surg Radiol Anat*. 2009;31:631–639.
9. Ludolph I, Horch RE, Arkudas A, et al. Enhancing safety in reconstructive microsurgery using intraoperative indocyanine green angiography. *Front Surg*. 2019;6:39.
10. Hayashi A, Yoshizawa H, Tanaka R, et al. Intraoperative use of indocyanine green fluorescence angiography during distally based radial artery perforator flap for squamous cell carcinoma of the thumb. *Plast Reconstr Surg Glob Open*. 2015;3:e310.
11. Chu W, Chennamsetty A, Toroussian R, et al. Anaphylactic shock after intravenous administration of indocyanine green during robotic partial nephrectomy. *Urol Case Rep*. 2017;12:37–38.
12. Lawson R. Implications of surface temperatures in the diagnosis of breast cancer. *Can Med Assoc J*. 1956;75:309–311.
13. Arai K, Fukuda O. [Clinical application of thermometers and thermography in plastic surgery]. *Keisei Geka*. 1968;11:239–250.
14. Sheena Y, Jennison T, Hardwicke JT, et al. Detection of perforators using thermal imaging. *Plast Reconstr Surg*. 2013;132:1603–1610.
15. Muntean MV, Strilciuc S, Ardelean F, et al. Using dynamic infrared thermography to optimize color Doppler ultrasound mapping of cutaneous perforators. *Med Ultrason*. 2015;17:503–508.
16. Hardwicke JT, Osmani O, Skillman JM. Detection of perforators using smartphone thermal imaging. *Plast Reconstr Surg*. 2016;137:39–41.

17. Suphachokauychai S, Kiranantawat K, Sananpanich K. Detection of perforators using smartphone thermal imaging. *Plast Reconstr Surg Glob Open*. 2016;4:e722.
18. Paul SP. Using a thermal imaging camera to locate perforators on the lower limb. *Arch Plast Surg*. 2017;44:243–247.
19. Konczalik W, Nikkhah D, Mosahebi A. Applications of Smartphone thermal camera imaging system in monitoring of the deep inferior epigastric perforator flap for breast reconstruction: applications of smartphone thermal camera.. *Microsurgery*. 2017;37:457–458.
20. Patel SS, Homsy C, Atamian EK, et al. Thermal imaging facilitates design of a keystone perforator island flap for a myxofibrosarcoma resection reconstruction: case report. *Plast Reconstr Surg Glob Open*. 2019;7:e2359.
21. Cruz-Segura A, Cruz-Domínguez MP, Jara LJ, et al. Early detection of vascular obstruction in microvascular flaps using a thermographic camera. *J Reconstr Microsurg*. 2019;35:541–548.
22. Pereira N, Valenzuela D, Mangelsdorff G, et al. Detection of perforators for free flap planning using smartphone thermal imaging: a concordance study with computed tomographic angiography in 120 perforators. *Plast Reconstr Surg*. 2018;141:787–792.
23. Muntean MV, Achimas-Cadariu PA. Detection of perforators for free flap planning using smartphone thermal imaging: a concordance study with computed tomographic angiography in 120 perforators. *Plast Reconstr Surg*. 2018;142:604e.
24. Hennessy O, Potter SM. The use of infrared thermography in the assessment of free flap perforators in autologous breast reconstruction: a systematic review. *JPRAS Open*. 2020;23:60-70.
25. Vardasca R, Magalhaes C, Silva P, et al. Are the IR cameras FLIR ONE suitable for clinical applications? *Thermol Int*. 2019;29:95–102.
26. Wilson SB, Spence VA. Dynamic thermographic imaging method for quantifying dermal perfusion: potential and limitations. *Med Biol Eng Comput*. 1989;27:496–501.
27. Itoh Y, Arai K. Use of recovery-enhanced thermography to localize cutaneous perforators. *Ann Plast Surg*. 1995;34:507–511.
28. de Weerd L, Mercer JB, Setså LB. Intraoperative dynamic infrared thermography and free-flap surgery. *Ann Plast Surg*. 2006;57:279–284.
29. de Weerd L, Weum S, Mercer JB. The value of dynamic infrared thermography (DIRT) in perforatorselection and planning of free DIEP flaps. *Ann Plast Surg*. 2009;63:274–279.
30. de Weerd L, Mercer JB, Weum S. Dynamic infrared thermography. *Clin Plast Surg*. 2011;38:277–292.
31. de Weerd L, Weum S, Mercer JB. Locating perforator vessels by dynamic infrared imaging and flow Doppler with no thermal cold challenge. *Ann Plast Surg*. 2014;72:261.
32. de Weerd L, Weum S, Mercer JB. Detection of perforators using thermal imaging. *Plast Reconstr Surg*. 2014;134:850e–851e.
33. Weum S, Lott A, de Weerd L. Detection of perforators using smartphone thermal imaging. *Plast Reconstr Surg*. 2016;138:938e–940e.
34. Weum S, Mercer JB, de Weerd L. Evaluation of dynamic infrared thermography as an alternative to CT angiography for perforator mapping in breast reconstruction: a clinical study. *BMC Med Imaging*. 2016;16:43.
35. Thiessen FEF, Tondu T, Cloostermans B, et al. Dynamic infrared thermography (dirt) in diep-flap breast reconstruction: a review of the literature. *Eur J Obstet Gynecol Reprod Biol*. 2019;242:47–55.